CCFE-PR(17)48

S. C. Chapman, P. T. Lang, R. O. Dendy, L. Giannone, N. W. Watkins,
and ASDEX 4 Upgrade Team

Global control system-plasma synchronization and naturally occurring edge localized modes in the ASDEX Upgrade tokamak

Global control system-plasma synchronization and naturally occurring edge localized modes in the ASDEX Upgrade tokamak

S. C. Chapman[1], P. T. Lang[2], R. O. Dendy[3,1], L. Giannone[2], N. W. Watkins[1,4,5], and ASDEX 4 Upgrade Team[2]

[1]Centre for Fusion, Space and Astrophysics, Department of Physics, Warwick University, Coventry CV4 7AL, UK
[2]Max-Planck-Institut für Plasmaphysik, Garching Germany
[3]CCFE, Culham Science Centre, Abingdon, Oxfordshire OX14 3DB, UK
[4]Centre for Analysis of Time Series, London School of Economics, London WC2A 2AE, UK
[5]Faculty of Mathematics, Computing and Technology, Open University, Milton Keynes, UK

Global control system-plasma synchronization and naturally occurring edge localized modes in the ASDEX Upgrade tokamak

S. C. Chapman[1], P. T. Lang[2], R. O. Dendy[3,1], L. Giannone[2], N. W. Watkins[1,4,5], ASDEX Upgrade Team[2]

EUROfusion Consortium, JET, Culham Science Centre, Abingdon OX14 3DB, UK

[1]*Centre for Fusion, Space and Astrophysics, Department of Physics, Warwick University, Coventry CV4 7AL, UK*

[2]*Max-Planck-Institut für Plasmaphysik, Garching Germany*

[3]*CCFE, Culham Science Centre, Abingdon, Oxfordshire OX14 3DB, UK*

[4]*Centre for Analysis of Time Series, London School of Economics, London WC2A 2AE, UK*

[5]*Faculty of Mathematics, Computing and Technology, Open University, Milton Keynes, UK*

Intro Paragraph

The ITER tokamak needs[1-3] to sustain a plasma in a regime of high energy confinement (H-mode[4-6]) to exceed fusion breakeven where power output exceeds input. H-mode plasmas are typically unstable to edge localised modes[7-10] (ELMs), in which plasma escapes and strikes the plasma facing components. Scaled up to ITER, the energy released by ELMs can cause critical damage[2,8] and needs to be addressed to achieve sustainable breakeven. Proposed methods for ELM control[11-18] include externally triggering smaller, more frequent ELMs by injecting pellets[17,18] of frozen deuterium that modify the plasma edge, or by externally applying magnetic kicks[11,14] by pulsing the current in toroidal magnetic field coils near the plasma boundary. Maintaining a steady state plasma requires active control[19] and this control system includes these global field coils. The standard paradigm is that the control system acts on a relatively short timescale to restore the plasma steady state following an instability such as an ELM. We find that under certain conditions the plasma transitions into a state in which the control system current in these field coils continually oscillates and is synchronized with oscillations in the plasma edge position and several characteristic plasma parameters such as total MHD energy. These synchronous oscillations have a one-to-one correlation with the naturally occurring ELMs; the ELMs all occur when the control system coil current is around a specific phase. In this synchronous state, there is a continual non-linear feedback between the active control system and the global plasma dynamics that is intrinsic to the natural ELMing process. This supports the new paradigm[21-23] that the nonlinear feedback between plasma and control system is an intrinsic part of the cyclic dynamics of naturally occurring ELMs for which there is evidence on JET[20-23]. Real time knowledge of the control system signal phase indicates future times when ELM occurrence is more likely.

Main Text

Edge localized modes[7-10] (ELMs) are intense, short duration relaxation events observed in high confinement H-mode regimes in tokamak plasmas. Typically, in present day devices a few hundred ELMs occur in the quasi-stationary phase of H-mode plasmas. Each ELM releases particles and energy which load the plasma facing components; scaled up to ITER[1], the largest such loads would be unacceptable[2,3]. In addition, ELMs are key in removing impurities from the plasma which must also be achieved in a controllable manner. Thus ELM prediction, mitigation and control[11-18] are central to magnetic confinement fusion (MCF) research. The peeling-ballooning MHD instability of the plasma edge is believed to underlie ELM initiation[24-26], however a comprehensive model for the birth-to-death ELM cycle is not yet available. Low dimensional features in the overall ELMing process have been observed in JET[27].

Empirically, longer waiting times between one ELM and the next correlate with larger ELM amplitudes[9], so that proposals for mitigation include externally triggering, or pacing, many smaller, more benign ELMs. This can be achieved by modifying the conditions at the edge by injecting frozen deuterium pellets[16-18] which quickly ionise. Successful triggering conditions depend on plasma and pellet parameters[17-18]. Externally applied vertical magnetic kicks[11,14] are also used to pace ELMs, they exert a force on the plasma which itself carries a large toroidal current (see the schematic ED Fig. 1). These magnetic kicks are implemented by inducing large scale plasma perturbations by pulsing the current in toroidal field coils that encircle the plasma. These field coils are also the vertical part of the active control system essential to maintaining the plasma in a global steady state[19]. Active control of the plasma is achieved by real-time monitoring of the plasma including changes in global plasma shape, current, position and velocity. The control system takes these inputs, and one of its outputs is to apply voltages to the field coils. This modifies the current in the field coils, generating inductive magnetic fields that react back on the plasma.

This prompts the new hypothesis[20-23]: that the nonlinear feedback between plasma and control system can be a substantial part of the natural dynamics of ELMs which are naturally occurring. If such a relationship between the control system and naturally occurring ELMs exists, then we would anticipate that under certain conditions the coupled control system and global plasma dynamics that governs natural ELM occurrence should access a state in which they are fully synchronized. We report the observation of just such a dynamics here.

We study in detail ELM occurrence in the steady state flat-top of H-mode ASDEX Upgrade (AUG) plasmas (the experiment details are given in the SI and ED). The ELM occurrence time is identified (see Methods) from an ELM monitor, the rise in the thermionic current observed at a tile in the divertor region. We will focus on high time resolution (50 microsecond, the same as for the ELM monitor) global signals (see the schematic, ED Fig 1): (i) the current in the field coils (I_C^u, I_C^l), which are actively used for vertical stabilization of the plasma by the control system; (ii) total magnetohydrodynamic field and plasma energy

(W_{MHD}); (iii) the location of the outboard edge of the plasma (R_{out}) and (iv) the line of sight integrated plasma density ($\bar{n}_e$). In ASDEX plasma 30416 we have found a transition to synchronous dynamics just after the electron cyclotron resonant heating (ECRH) is switched off at t=6.2 s, this dynamics persists for 0.7 s, after which the plasma terminates. Overview time-series are given in ED Fig 2 and 3. This interval of synchronous dynamics is quite robust, persisting whilst two pellets are injected during this interval which can be seen to enhance the line of sight plasma density. Fig 1 plots a time sub-interval of this global synchronous dynamics.

We use the ELM monitor signal (see methods) to identify times associated with the ELM onset and crash. ELM onset can be seen at the time when the ELM monitor is sharply rising. We identify this onset time (t_R,open red circles throughout Fig 1) where the ELM monitor is just about to cross a threshold which is one standard deviation above its background (green line). The end of the ELM crash is identified as the time when the ELM monitor falls below the same threshold, indicated by the blue stars. To test the idea that the control system is in continual feedback with the plasma-ELMing process and so influences ELM onset, as well as responding to ELM crash, we also identify a time (t_B) which is 350 microseconds before ELM onset t_R, indicated on all panels of Fig 1 by filled blue circles. In Fig 1 the ELM crash can be seen as a sharp drop in total plasma energy (W_{MHD}) and an inward movement of the plasma edge (R_{out}); we can see that the time (t_B) is when the plasma MHD energy and edge position are at their peak values; the ELM crash has not yet occurred. The current in the control system field coils, the I_C^u signal, is roughly oscillatory and the ELMs tend to occur when it is at a particular phase of its oscillation. The control system field coil current (I_C^u) instantaneous phase plotted in Fig 1, $\phi(t)$, is obtained via Hilbert transform such that the signal $S(t) = A(t)\exp[i\phi(t)]$ (see Methods). Phase is defined relative to a single reference value, here, the average instantaneous phase of the signal at the time of the ELMs in the time window. In Figure 2 we plot a histogram of the I_C^u phases at the ELM onset times (upper panel, t_R) and 350 μs before this, (lower panel, t_B), and we calculate Rayleigh's R number at t_R and t_B. A value of $R = 1$ indicates that all phases are exactly aligned, for the interval $t = 6.4 - 7.1$ seconds where we identify synchronous dynamics we find $R(t_R) = 0.91$ and $R(t_B) = 0.88$. We find similar phase bunching in I_C^l with slightly lower R values (see ED). Importantly, we see strong phase synchronization when ELM onset has begun, and also at a time before it; thus this phase relationship is not simply due to the response of the control system to each ELM crash.

The synchronized dynamics of control system and plasma is shown in Fig 3. The left hand panels plot the mean subtracted location of the plasma outer edge (R_{out}) and the total plasma MHD energy (W_{MHD}) versus the (mean subtracted) current in the control system field coils (

I_C^u) for the interval $t = 6.4 - 7.1$s where there is synchronous dynamics. The signal values just before each ELM, at time t_B, are again plotted with blue circles. For each ELM, the plasma and control system together execute a cycle: (a) there is a build up during which the plasma total energy increases with little change in the outer edge location whilst the current in the control system coils becomes more negative followed by (b) the ELM crash, in which both total energy sharply drops and plasma edge moves rapidly inward whilst the control system current does not change significantly then (c) a recovery in which the control system becomes more positive, the plasma edge moves outwards and the total energy does not change significantly. The control system field coil current (I_C^u) phase orders the global plasma dynamics as captured by the total plasma energy and edge location; the right hand panels plot these quantities versus I_C^u signal phase. Just before the ELM onset, at time t_B (blue circles) the I_C^u phases are clustered about zero and we can see that the build up (a) and recovery (c) occur over two halves of the (I_C^u) control system current cycle. In this synchronous state, there is a continual non-linear feedback between global plasma dynamics and control system that is intrinsic to the natural ELMing process. During this time interval, pellets are injected into the plasma and these can be seen to modify the plasma conditions- the plasma line-of sight density ($\bar{n}_e$, see ED Figure 2) which is enhanced by about 7%. This does not perturb the dynamics of the I_C^u signal phase which suggests that this is attractive, limit cycle dynamics.

On JET we previously found a class of prompt[20-22] natural ELMs in which the plasma's own response to the previous ELM provides the necessary global plasma dynamics to precipitate the next ELM. We would thus expect that fully synchronous dynamics should occur under certain conditions where coupling between the control system and perturbations in the plasma, become synchronized[28-30] and their synchronous oscillations coincide with the occurrence times of all the natural ELMs. We have identified just such a synchronous dynamics here. This suggests a paradigm shift in which the control system-plasma feedback can be a significant part of the natural ELMing process. This may have potential to be developed as a direct tool for ELM pacing and hence mitigation. In this synchronous dynamics, the ELM occurrence times and energies both become more predictable.

Methods

The experiments

We present detailed analysis of AUG discharge 30416. Plasma 30416 has a flat-top H-mode with ECRH heating of 1.2 MW at 140 GHz which ends at $t = 6.2s$ at which time we see a transition to a synchronous state. In 30416 the plasma parameters are $I_p = 0.8MA, B_T = 2.5T, P_{NBI} = 2.5MW$ and we analyse the synchronous interval 6.4-7.1s, and compare with an earlier interval in the same plasma of the same duration at 5.5-6.2s.

ELM occurrence times are inferred from an ELM monitor which is the thermionic current in a tile in the divertor region. The control system dynamics is inferred from the instantaneous analytic phase of high time resolution signals I_C^u and I_C^l which are the current in the toroidal field coils for active vertical control of the plasma. The global plasma state is inferred from the total MHD energy (W_{MHD}) and the outboard edge location (R_{out}). These signals are sampled at 50 microsecond time resolution.

Determination of ELM occurrence time

We determine the ELM occurrence times from the ELM monitor signal as follows. We find a 300pt rloess running mean *R(t)* which down-weights outliers. We then subtract this running mean from the Ipolsola signal giving *S(t)=I(t)-R(t)*. We take as a threshold TH(t) the running mean plus one standard deviation of *S(t)*. We then can usefully identify three time points in an ELM: (i) the data point before the first up-crossing time when *S(t)>TH(t),* t_R (red open circles) (ii) a time just before the beginning of the ELM which is $t_B = t_R - dt$ (blue filled circles) and *dt* is determined by inspection of the ELM monitor and W_{MHD} signals, for the plots here this is 7 pts ($dt = 350\mu s$) and (iii) the data point before the first down crossing time *S(t)<TH(t)* following the ELM monitor peak, (black star) t_F. To avoid detection of multiple crossings due to noise we work with *S(t)* which is a 5 point running average of the original signal. These can be seen to independently identify both the sharp energy drop in W_{MHD} and the change in R_{out}. We use the same symbols on all the panels.

Determination of pellet occurrence time

Frozen Deuterium pellets are injected into the plasma and the injection times can be found from peaks in a pellet ablation radiation monitor signal and their impact on the plasma is seen in the line-of-sight plasma density ($\bar{n}_e$), see ED Figure 2.

Instantaneous amplitude and phase of the control system field coil currents

A real valued signal $S(t)$ and its Hilbert transform, $H(t)$ together define the analytic signal $S(t) + iH(t) = A(t)\exp[i\phi(t)]$ with instantaneous amplitude $A(t)$ and phase $\phi(t)$; so that the signal is represented by a single mode with time dependent amplitude and frequency. The I_C^u and I_C^l signals have a time-varying baseline. We first subtract a 1000 pt running rloess mean. The analytic amplitude and phase is then obtained by Hilbert transform of this signal. The (mean subtracted) signal can have a strongly varying amplitude as the response to an ELM is much larger than other components in the signal that are of interest. Before obtaining the analytic phase by Hilbert transform we non-linearly transform these signals by dividing by the square root of the absolute magnitude. We have verified that the phase relationships determined here are robust against this transformation, that is we obtain the same phase

relationships, in particular, the result that ELMs occur at the same phase in these signals, is obtained whether or not this transformation is applied.

These methods are only effective if the signals have good signal/noise and if the mean of the signal does not vary too rapidly. The high rate of change of instantaneous phase with time of these signals requires well defined ELM occurrence times in order to cleanly determine any phase relationship. Phase is always determined from some reference value, here we use as our reference the average phase of the signal at the time of all ELMs in a given time window. All the ELMs in a given analysed time window then have phases given relative to this same reference phase value.

Circular statistics and surrogates

We use the Rayleigh test to quantify the extent to which the instantaneous phases of the field coil at a particular time before each ELM, for all ELMs in a given time window, are aligned, and the statistical significance of any such alignment. Using the procedure described above, we determine the instantaneous phases $\phi_k(t)$, for the $k = 1..N$ ELMs in the steady flat top of a given plasma. If each phase is represented by a unit vector $\mathbf{r}_k = (x_k, y_k) = (\cos\phi_k(t), \sin\phi_k(t))$ then a measure of their alignment is given by the magnitude of the vector sum, normalized to N. This is most easily realized if we use unit magnitude complex variables to represent the $\mathbf{r}_k = \exp[i\phi_k(dt)]$. The mean phase angle $\bar{\phi}$ is then given by:

$$\sum_{k=1}^{N} \mathbf{r}_k = re^{i\bar{\phi}}$$

and the Rayleigh number is the magnitude of the sum:

$$R = \frac{1}{N}\left|\sum_{k=1}^{N} \mathbf{r}_k\right| = \frac{r}{N}$$

If $R = 1$ the phases are completely aligned. We obtain $R(t)$ both at the ELM time t_R and just before, at t_B. An estimate of the *p*-value under the null hypothesis that the vectors are uniformly distributed around the circle is:

$$p = \exp\left[\sqrt{1 + 4N + 4N^2(1 - R^2)} - (1 + 2N)\right]$$

This null hypothesis can be rejected with 95% confidence for $p < 0.05$; here we found $p < 10^{-10}$ for the phases plotted in Fig 2.

Figure Captions

Figure 1: ELM- control system synchronous dynamics. Time traces are plotted for a short time window within the interval t=6.4-7.1 s of synchronous dynamics in plasma 30416. From top to bottom we plot with black traces: the edge position (R_{out}), the current in a tile in the divertor region (ELM monitor), the total MHD energy in the plasma (W_{MHD}), the current in the upper vertical control system coil (I_C^u), its analytic phase, and the plasma line of sight density ($\bar{n}_e$). ELM occurrence times are determined from the ELM monitor signal. The ELM onset time t_R (open red circles) and end time t_F (blue star) are at the data points just before the ELM monitor upcrossing, and downcrossing of a threshold (green line) which is one standard deviation away from the signal running baseline (red line). The filled blue circles are at a time just before the start of the ELM crash, $t_B = t_R - dt$ (here, $dt = 350\mu s$).

Figure 2 Quantifying the phase alignment. Circular statistics (see methods) for the interval t=6.4-7.1 s of synchronous dynamics in plasma 30416. Histograms of instantaneous phase of the I_C^u signal are plotted at the ELM onset t_R (upper panel) and just before at t_B (lower panel), the Rayleigh number (see methods) is given for each; if at a given time before the ELM, the signal was always at exactly the same phase, then one would obtain $R(t) = 1$. The *p*-value for the null hypothesis that the phases are uniformly distributed can be rejected with 95% confidence for $p < 0.05$, here $p < 10^{-10}$.

Figure 3 ELM-control system limit cycle. The location of the plasma outer edge (R_{out}, upper panels) and the total plasma MHD energy (W_{MHD}, lower panels) are plotted versus the current in the control system field coils (I_C^u, left panels) and its phase (right panels). Except for the I_C^u phase, the plotted traces have their respective running means subtracted, and the signals are plotted for the full interval of synchronous dynamics t=6.4-7.1s (grey dots). One cycle of this dynamics, that is, from one ELM to the next, is overplotted (solid black line). For each ELM, the signals at the time just before ELM onset t_B are plotted (blue filled circles). The dynamics is a build up phase (a) terminating in ELM onset, followed by the ELM crash (b) and then recovery (c).

Acknowledgements

S.C.C and N.W.W acknowledge the visitor programmes of the MPIPKS, Dresden, and the PIK Potsdam. This work has been carried out within the framework of the EUROfusion Consortium and has received funding from the Euratom research and training programme 2014-2018 under grant agreement number 633053, and from the RCUK Energy Programme [grant number EP/P012450/1]. The views and opinions expressed herein do not necessarily reflect those of the European Commission.

Author Contributions

SCC wrote the paper with inputs from all authors. SCC and NWW designed the analysis and SCC performed the analysis. PTL performed the experiments. ROD advised on ELM and MCF plasma phenomenology. LG and PTL identified the relevant diagnostics.

Author Information

Corresponding author: S C Chapman S.C.Chapman@warwick.ac.uk.

Data deposition

References

1. Shimada, M., Campbell, D. J., Mukhovatov, V., Fujiwara, M., Kirneva, N., Lackner, K., Nagami, M., Pustovitov, V. D., Uckan, N., Wesley, J. *et al*. Progress of the ITER physics basis: overview and summary. *Nucl. Fusion* **47,** S1-S17 (2007).

2. Hawryluk, R. J., Campbell, D. J., Janeschitz, G., Thomas, P. R., Albanese, R., Ambrosino, R., Bachmann, C., Baylor, L., Becoulet, M., Benfatto, I., Bialek J., Boozer, A. *et al*. Principal physics developments evaluated in the ITER design review. *Nucl. Fusion* **49,** 065012 (2009).

3. Kessel, C. E., Campbell, D., Gribov, Y., Saibene, G., Ambrosino, G., Budny, R. V., Casper, T., *et al*. Development of ITER 15MA ELMy H-mode inductive scenario. *Nucl. Fusion* **49,** 085034 (2009).

4. Wagner, F., Becker, G., Behringer, K., Campbell, D., Eberhagen, A., Engelhardt, W, Fussmann, G. et al. Regime of improved confinement and high beta in neutral-beam-heated divertor discharges of the ASDEX tokamak. *Phys. Rev. Lett*. **49,** 1408-1412 (1982).

5. Keilhacker, M., Becker, G., Berrnhardi, K., Eberhagen, A., ElShaer, M., Fussmann, G. *et al*. Confinement studies in L and H-type ASDEX discharges. *Plasma Phys. Controlled Fusion* **26,** 49-63 (1984).

6. Wagner, F. A quarter-century of H-mode studies. *Plasma Phys. Controlled Fusion* **49,** B1-B33 (2007).

7. Zohm, H. Edge localised modes (ELMs). *Plasma Phys. Controlled Fusion* **38,** 105-128 (1996).

8. Loarte, A., Saibene, G., Sartori, R., Campbell, D., Becoulet, M., Horton, L., Eich, T., Herrmann, A., Matthews, G., Asakura, N., Chankin, A., Leonard, A., Porter, G., Federici, G., Janeschitz, G., Shimada, M., & Sugihara, M. Characteristics of Type I ELM energy and particle losses in existing devices and their extrapolation to ITER. *Plasma Phys. Controlled Fusion* **45,** 1549-1569 (2003).

9. Kamiya, K., Asakura, N., Boedo, J., Eich, T., Federici, G., Fenstermacher, M., Finken, K., Herrmann, A., Terry, J., Kirk, A., Koch, B., Loarte, A., Maingi, R., Maqueda, R., Nardon, E., Oyama, N. & Sartori, R. Edge localized modes: recent experimental findings and related issues. *Plasma Phys. Controlled Fusion* **49**, S43-S62 (2007).

10. Leonard, A.W. Edge localised modes in tokamaks, *Phys*. *Plasmas* **21,** 090501 (2014)

11. Lang, P. T., Degeling, A. W., Lister, J. B., Martin, Y. R., McCarthy, P. J., Sips, A. C. C., Suttrop, W., Conway, G. D., Fattorini, L., Gruber, O., Horton, L. D., Hermann, A., Manso, M. E., Maraschek, M., Mertens, V., Mueck, A., Schneider, W., Sihler, C., Treutterer, W., Zohm, H. & ASDEX Upgrade Team. Frequency control of type-I ELMs by magnetic triggering in ASDEX Upgrade. *Plasma Phys. Controlled Fusion* **46,** L31–L39 (2004).

12. Evans, T. E., Moyer, R. E., Burrell, K. H., Fenstermacher, M. E., Joseph, I., Leonard, A. W., Osborne, T. H., Porter, G. D., Scghaffer, M. J., Snyder, P. B., Thomas, P. R., Watkins, J. G. & West, W. P. Edge stability and transport control with resonant magnetic perturbations in collisionless tokamak plasmas. *Nature Phys.* **2,** 419-423 (2006).

13. Liang, Y., Koslowski, H. R., Thomas, P. R., Nardon, E., Alper, B., Andrew, P., Andrew, Y. *et al*. Active control of type-I edge-localized modes with $n = 1$ perturbation fields in the JET tokamak. *Phys. Rev. Lett*. **98,** 265004 (2007).

14. de la Luna, E., Chapman, I. T., Rimini, F., Lomas, P. J., Saibene, G., Koechl, F., Sartori, R., Saarelma, S., Albanese, R., Flanagan, J., Understanding the physics of ELM pacing via vertical kicks in JET in view of ITER, *Nuc. Fusion*, **56**, 2, (2016)

15. Kirk, A., Harrison, J., Liu, Y., Nardon, E., Chapman, I. T., & Denner, P. Observations of lobes near the X-point in resonant magnetic perturbation experiments in MAST. *Phys. Rev. Lett.* **108,** 255003 (2012).

16. Baylor, L. R., Commaux, N., Jernigan, T. C., Brooks, N. H., Combs, S. K., Evans, T. E., Fenstermacher, M. E., Isler, R. C., Lasnier, C. J., Meitner, S. J., Moyer, R. A., Osborne, T. H., Parks, P. B., Snyder, P. B., Strait, E. J., Unterberg, E. A., Loarte, A., *Phys. Rev. Lett.* **110**, 245001, (2013)

17. Lang, P.T., Conway, G.D., Eich, T., Fattorini, L., Gruber, O., Günter, S., Horton, L., Kálvin, D. S., Kallenbach, A., Kaufmann, M., Kocsis, G., Lorenz, A., Manso, M.E., Maraschek, M., Mertens, V., Neuhauser, J., Nunes, I., Schneider, W., Suttrop, W., Urano, H., ASDEX Upgrade Team, ELM pace making and mitigation by pellet injection in ASDEX Upgrade, *Nuc. Fusion*, **44**, 665-677, (2004)

18. Lang, P.T., Neuhauser, J., Horton, L. D., Eich, T., Fattorini, L. Fuchs, J.C., Gehre, O., Herrmann, A., Ignácz, P., Jacobi, M., Kálvin, S., Kaufmann, M. , Kocsis, G., Kurzan, B., Maggi, C., Manso, M.E., Maraschek, M., Mertens, V., Mück, A., Murmann, H. D., Neu, R., Nunes, I., Reich, D., Reich, M., Saarelma, S., Sandmann, W., Stober, J., Vogl, U. , ASDEX Upgrade Team, ELM frequency control by continuous small pellet injection in ASDEX Upgrade, *Nuc. Fusion*, **43**, 1110-1120, (2003)

19. Treutterer, W., Cole, R., Lüddecke, K., Neu, G., Rapson, C. J., Raupp, G., Zasche, D., Zehetbauer, T., ASDEX Upgrade Discharge Control System — A real - time plasma control framework, Fusion Eng. Des. , 89, 146, (2014)

20. Chapman, S. C., Dendy, R. O., Todd, T.N., Watkins, N.W, Webster, A.J., Calderon, F. A., Morris, J. & JET-EFDA Contributors. Relationship of ELM burst times with divertor flux loop signal phase in JET. *Phys. Plasmas* **21**, 062302 (2014),

21. Chapman, S. C., Dendy, R. O., Webster, A. J., Watkins, N.W, Todd, T.N, Morris, J. & JET-EFDA Contributors. An apparent relation between ELM occurrence times and the prior

phase evolution of divertor flux loop measurements in JET. *Proc. 41st EPS Conference on Plasma Physics, Europhysics Conference Abstracts (European Physical Society*), Vol. **38F**, ISBN 2-914771-90-8, paper 101 http://ocs.ciemat.es/EPS2014PAP/pdf/P1.010.pdf (2014).

22. Chapman, S. C., Dendy, R. O., Todd, T. N., Watkins, N. W., Calderon, F. A., Morris, J. & JET Contributors. The global build-up to intrinsic ELM bursts seen in divertor full flux loops in JET. *Phys. Plasmas* **22,** 072506 (2015).

23 S. C. Chapman, R. O. Dendy, P. T. Lang, N. W. Watkins, F. Calderon, M. Romanelli, T. N. Todd and JET Contributors, The global build-up to intrinsic ELM bursts and comparison with pellet precipitated ELMs seen in JET, *Nuc. Fusion*, 57, 022017, (2017)

24. Snyder, P. B., Wilson, H. R. & Xu, X. Q. Progress in the peeling-ballooning model of edge localized modes: numerical studies of nonlinear dynamics. *Phys. Plasmas* **12,** 056115 (2005).

25. Connor, J. W., Edge-localized modes - physics and theory, PPCF 40, 531 (1998)

26. Saarelma, S., A Alfier, M N A Beurskens, R Coelho, H R Koslowski, Y Liang, I Nunes and JET EFDA contributors, MHD analysis of small ELM regimes in JET, PPCF 51, 035001 (2009)

27. Calderon, F. A., Dendy, R. O., Chapman, S. C., Webster, A. J., Alper, B., Nicol, R. M. & JET EFDA Contributors. Identifying low-dimensional dynamics in type-I edge-localised-mode processes in JET plasmas. *Phys. Plasmas* **20,** 042306 (2013).

28. Rosenblum, M .G., Pikovsky, A. S. & Kurths, J. Phase synchronisation of chaotic oscillators *Phys. Rev. Lett*. **76,** 1804-1807 (1996).

29. Pikovsky, A., Rosenblum, M. G. & Kurths, J. Synchronization: a universal concept in nonlinear sciences (Cambridge Univ. Press, 2003).

30. Schwabedal, J. T. C. & Pikovsky, A. S. Phase description of stochastic oscillations. *Phys. Rev. Lett.* **110,** 204102 (2013).

Figures

Figure 1

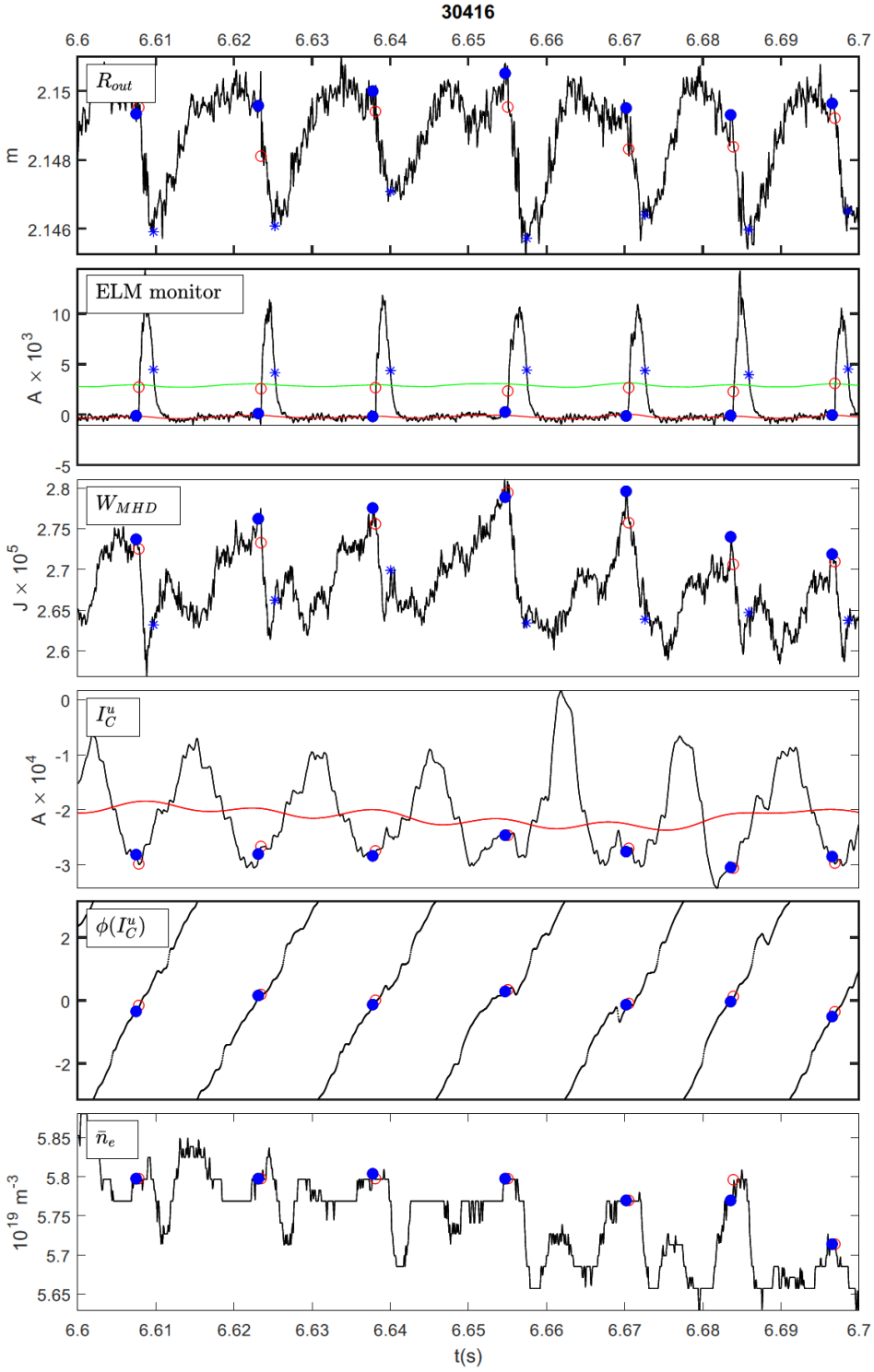

363 **Figure 2**

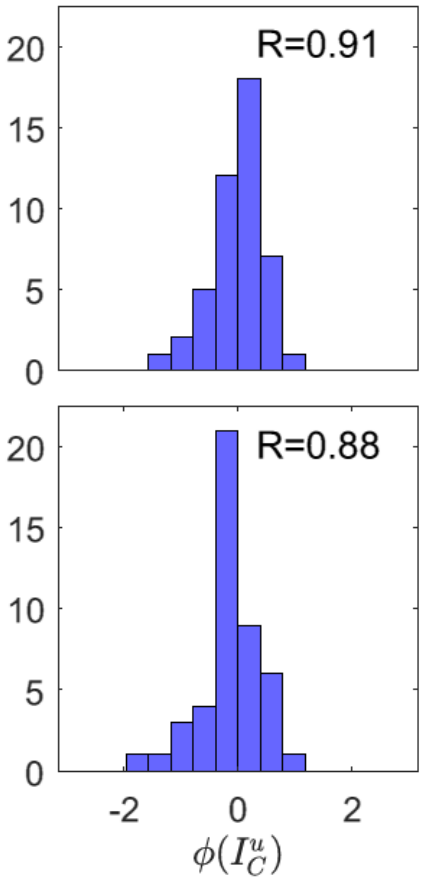

364

365

366

Figure 3

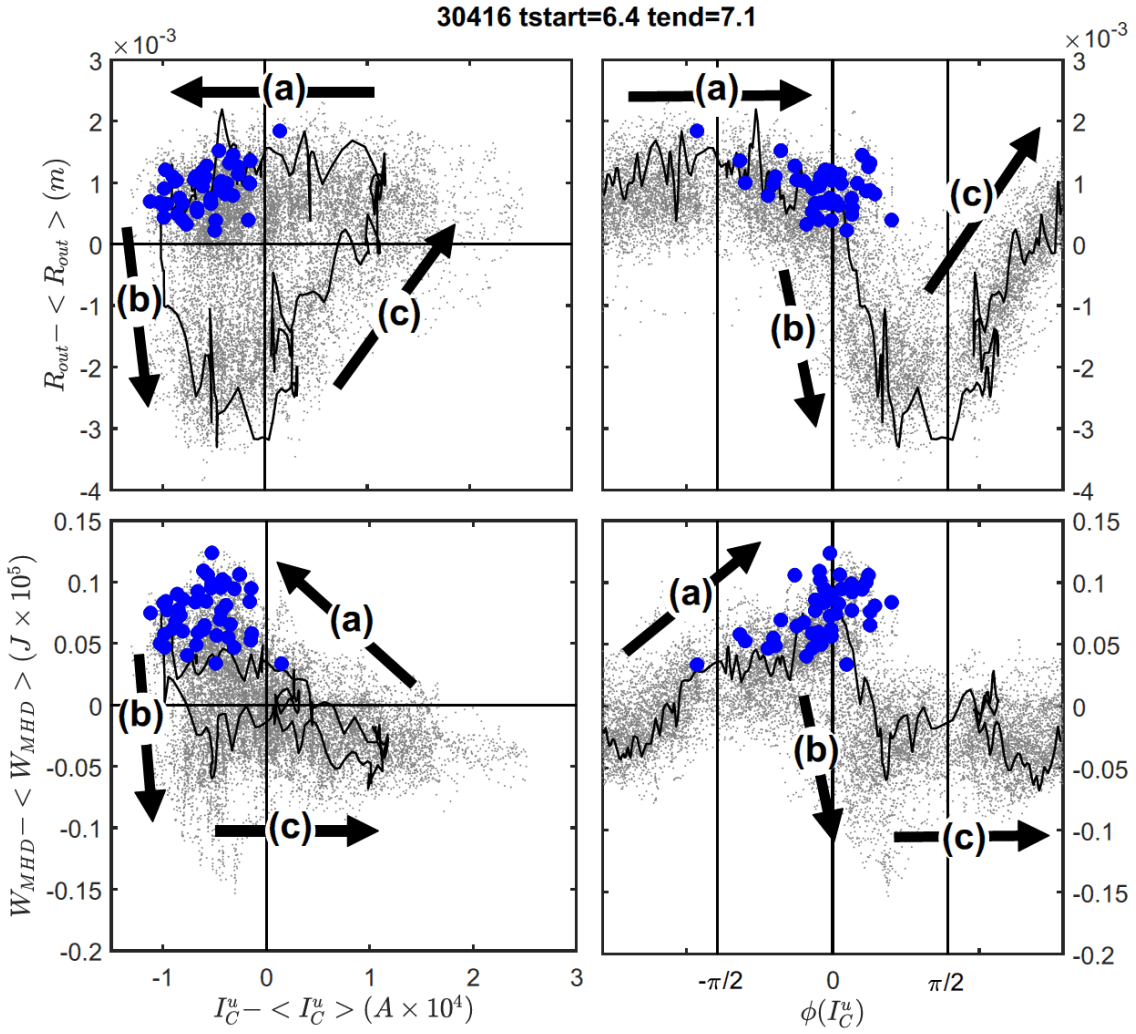
30416 tstart=6.4 tend=7.1
$\times 10^{-3}$
$R_{out} - < R_{out} > (m)$
$W_{MHD} - < W_{MHD} > (J \times 10^5)$
$I_C^u - < I_C^u > (A \times 10^4)$
$\phi(I_C^u)$
(a)
(b)
(c)
-π/2
0
π/2

Supplementary Information

We study in detail ELM occurrence in the steady state flat-top of H-mode ASDEX Upgrade plasmas. The ELM occurrence time is identified (see Methods) from an ELM monitor: the rise in the current observed at a tile in the divertor region. We focus on high time resolution (50 microsecond) global signals as shown in the schematic ED Figure 1: (i) the current in the fast radial field coils (I_C^u, I_C^l), which are actively used for vertical stabilization of the plasma by the control system; (ii) total magnetohydrodynamic field and plasma energy (W_{MHD}) (iii) location of the outboard edge of the plasma (R_{out}) (iv) plasma line of sight density ($\overline{n}_e$). In plasma 30416 the ECRH heating is switched off at t=6.2 s (see ED Figure 2) following which there is a transition to synchronous dynamics which persists for 0.7 s, after which the plasma ends (see ED Figure 3). This interval of synchronous dynamics is quite robust, persisting whilst two pellets are injected during this interval which can be seen to enhance the line of sight plasma density.

In ED Figures 5 and 6 we consider an interval earlier in the same plasma, for the same length of time interval (0.7s) for which we have found synchronous behaviour. Here the I_C^u phase is far less bunched, however it is not random, if we calculate Rayleigh's R excluding smaller ELMs we find alignment that is significant (R=0.55) but is not as strong as in the fully synchronised interval.

The energy released by ELMs as measured from the WMHD drop is plotted in ED Figure 7.

Extended Data Figures

ED Figure 1

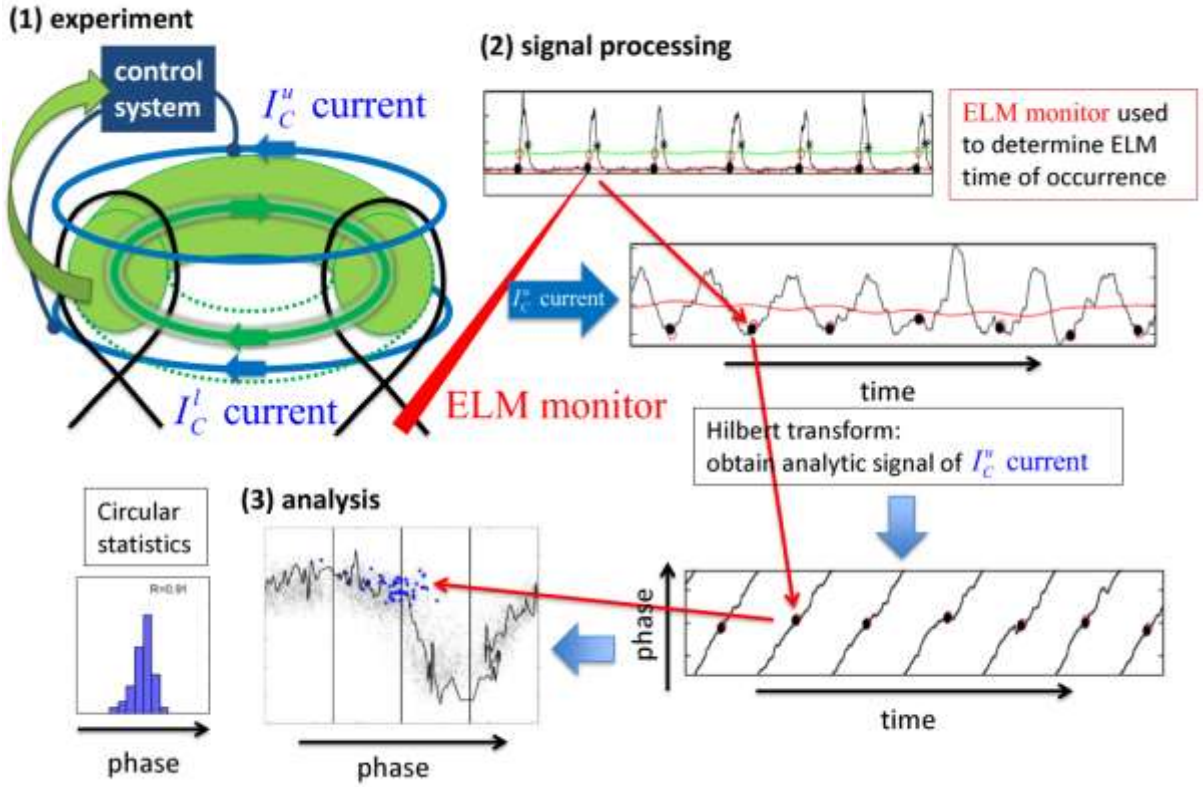

Schematic of the ASDEX plasma experiment and the analysis in this Letter. Counter-clockwise from top left: (1) experimental setup; (2) signal processing; (3) characterisation and statistical analysis. In (1), the plasma and its toroidal electric current (both green) are shown within twin poloidal projections (black) of the last closed toroidal magnetic flux surface, with the divertor region below the X-point. The plasma is maintained by a control system which takes as its inputs multiple signals which monitor changes in plasma position, plasma movement and changes in the magnitude and spatial distribution of the electric current density within it. The control system, as its output, applies voltages to system scale field coils including those used to correct vertical position, a subset of which are the toroidal radial field coils, we analyse the current in these coils (labelled I_C^l, lower, and I_C^u,upper, shown blue). Short duration edge localised modes (ELMs) cause loss of plasma particles which strike the material walls (not shown). This results in a reflux of neutral particles from the walls which, on entering the plasma and becoming ionised, give rise to the ELM monitor signal which is the thermo-electric current into an outer divertor tile, shown in red. In (2), the ELM monitor signal is used to determine ELM occurrence times, which can then be compared to the instantaneous amplitude and phase of the radial field coil signals, as well as other variables such as plasma edge position and total MHD energy that indicate the global plasma state. The I_C^u and I_C^l instantaneous amplitude and phase are determined by

constructing an analytic signal by performing a local Hilbert transform over the full time duration of the plasma. The information content of the analytic signal is optimal if it is obtained from a timeseries that is zero-crossing, this is achieved here by subtracting a locally determined mean as shown (see Methods).

Once the instantaneous amplitude and phase are determined, we then perform analysis (3) to quantify the degree of phase alignment, and to explore limit cycle dynamics.

ED Figure 2

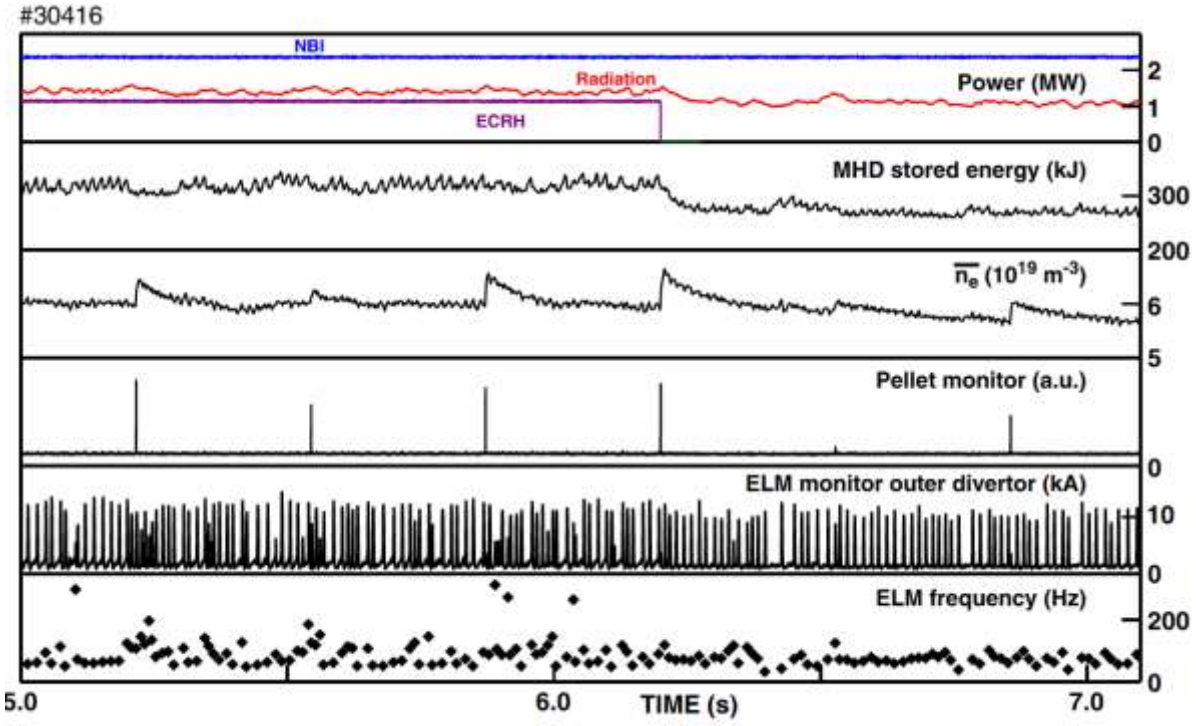

Time evolution of the experiment. Experimental plasma parameters are plotted for the latter part of plasma 30416. From the top panel we see that neutral beam injection (NBI) heating and plasma radiation are constant whereas electron cyclotron resonant heating (ECRH) is stepped down at t=6.2s. This results in a drop in total MHD stored energy (second panel). Pellets are injected throughout this interval, resulting in enhancements in line of sight integrated density (third panel) and spikes in the pellet monitor (fourth panel). ELM arrival times and frequency are indicated in the lower two panels.

ED Figure 3(a)

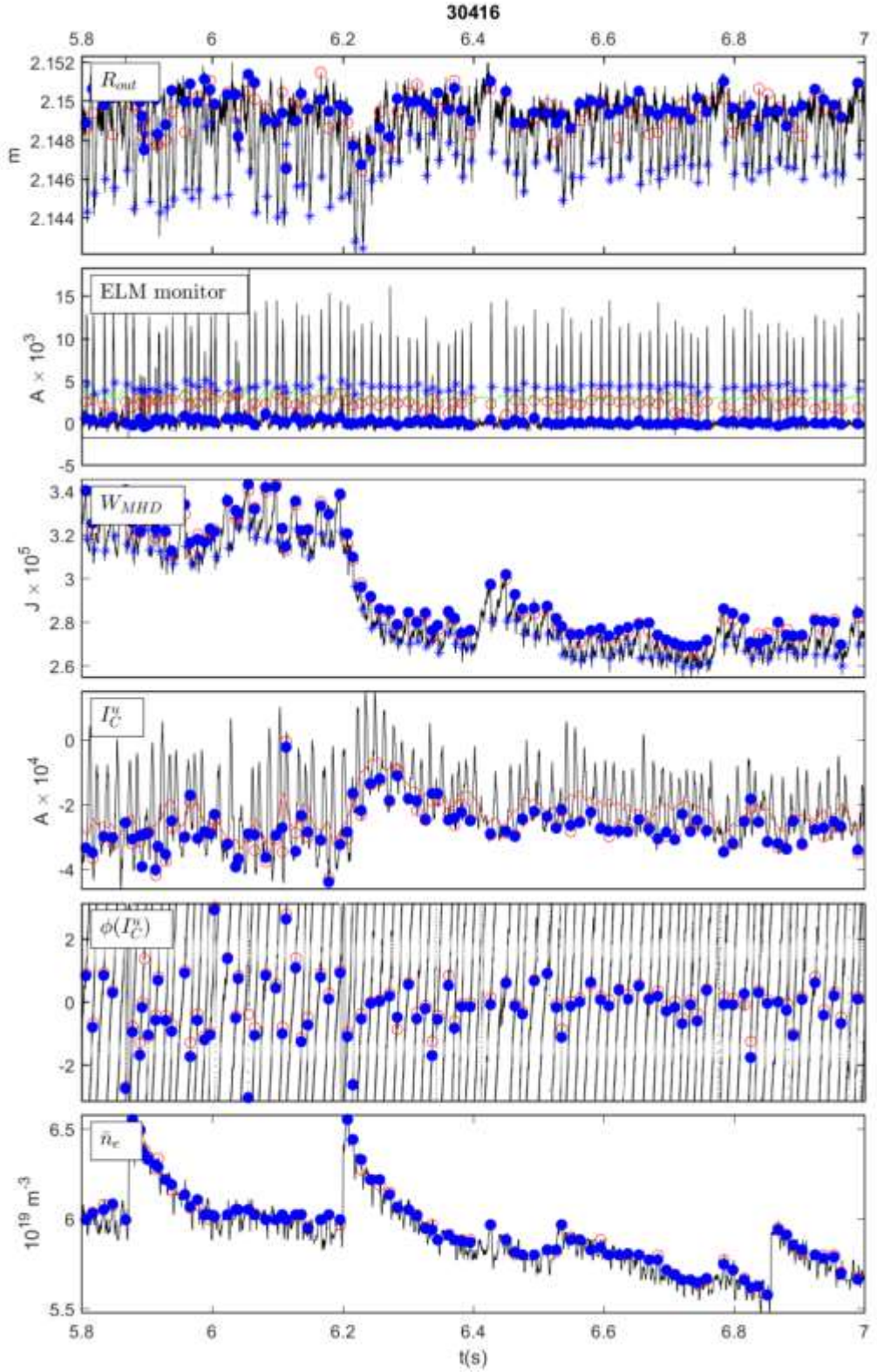
30416
R_{out}
m
ELM monitor
A × 10^3
W_{MHD}
J × 10^5
I_C^n
A × 10^4
$\phi(I_C^n)$
$\bar{n}_e$
10^19 m^-3
t(s)

40 **ED Figure 3(b)**

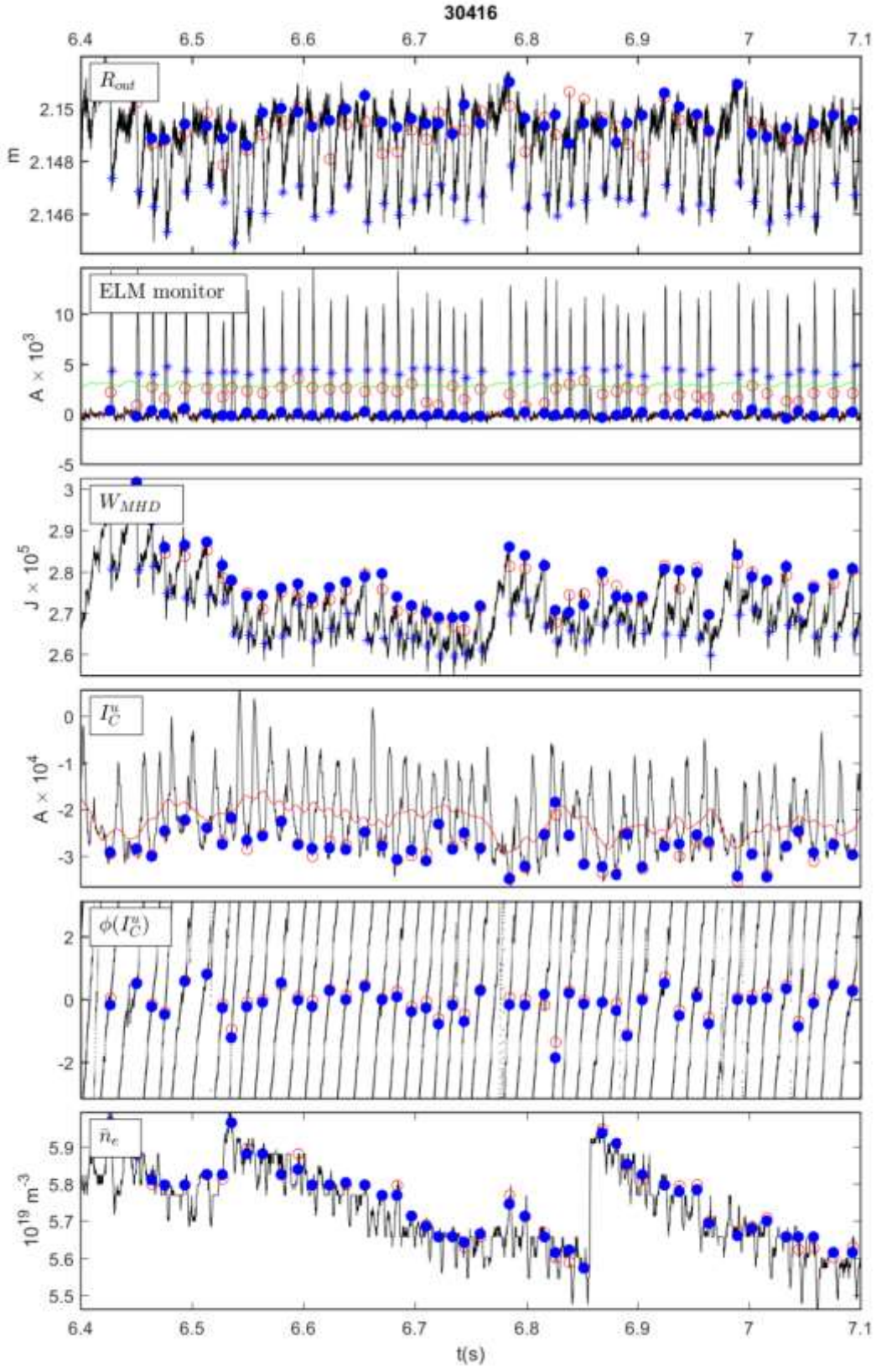

41

Overview plots of the transition to synchronous dynamics. Fig 3(a) plots a time interval showing the transition to synchronous dynamics and Fig 3(b) shows the full time interval in which synchronous dynamics occurs. From top to bottom we plot with black traces: the edge position (R_{out}), the current in a tile in the divertor region, the ELM monitor, the total MHD energy in the plasma (W_{MHD}), the current in the upper vertical control system coil (I_C^u), its analytic phase, and the plasma line of sight density ($\bar{n}_e$). ELM occurrence times are determined from the ELM monitor signal. The ELM onset time t_R (open red circles) and end time t_F (blue star) are at the data points just before the ELM monitor upcrossing and downcrossing of a threshold (green line) which is one standard deviation away from the signal running baseline (red line). The filled blue circles are at a time just before the start of the ELM crash, $t_B = t_R - dt$ (here, $dt = 0.35\mu s$).

In Fig 3(a) we can see a transition at t=6.2 s, the total MHD energy drops by about 6% and the I_C^u phases just before the ELM crash times become more aligned around zero. Fig 3(b) plots the interval t=6.4-7.1s over which we can see that the I_C^u phases just before the ELM crash times remain around zero, histograms for these phases are given in Fig 2 main text and below. This interval of synchronous dynamics is quite robust and persists whilst two pellets are injected during this interval enhancing the line of sight plasma density.

ED Figure 4

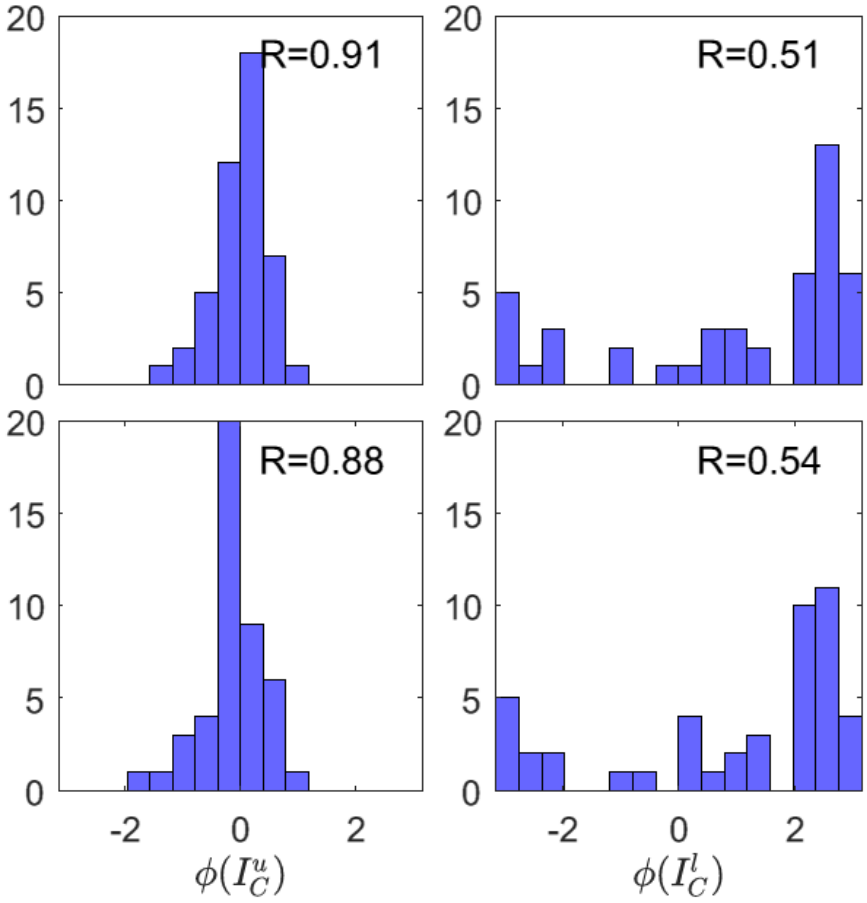

Histograms as in Figure 2 main text for both upper and lower control system field coils.

Circular statistics (see methods) for the interval t=6.4-7.1 s of synchronous dynamics in plasma 30416. Histograms of instantaneous phase of the I_C^u (left panels) and I_C^l (right panels) signals are plotted at the ELM onset t_R (upper panels) and just before at t_B (lower panels), the Rayleigh number (see methods) is given for each; if at a given time before the ELM, the signal was always at exactly the same phase, then one would obtain $R(t)=1$. The *p*-value for the null hypothesis that the phases are uniformly distributed can be rejected with 95% confidence for $p<0.05$, here $p<10^{-10}$.

77 **ED Figure 5**

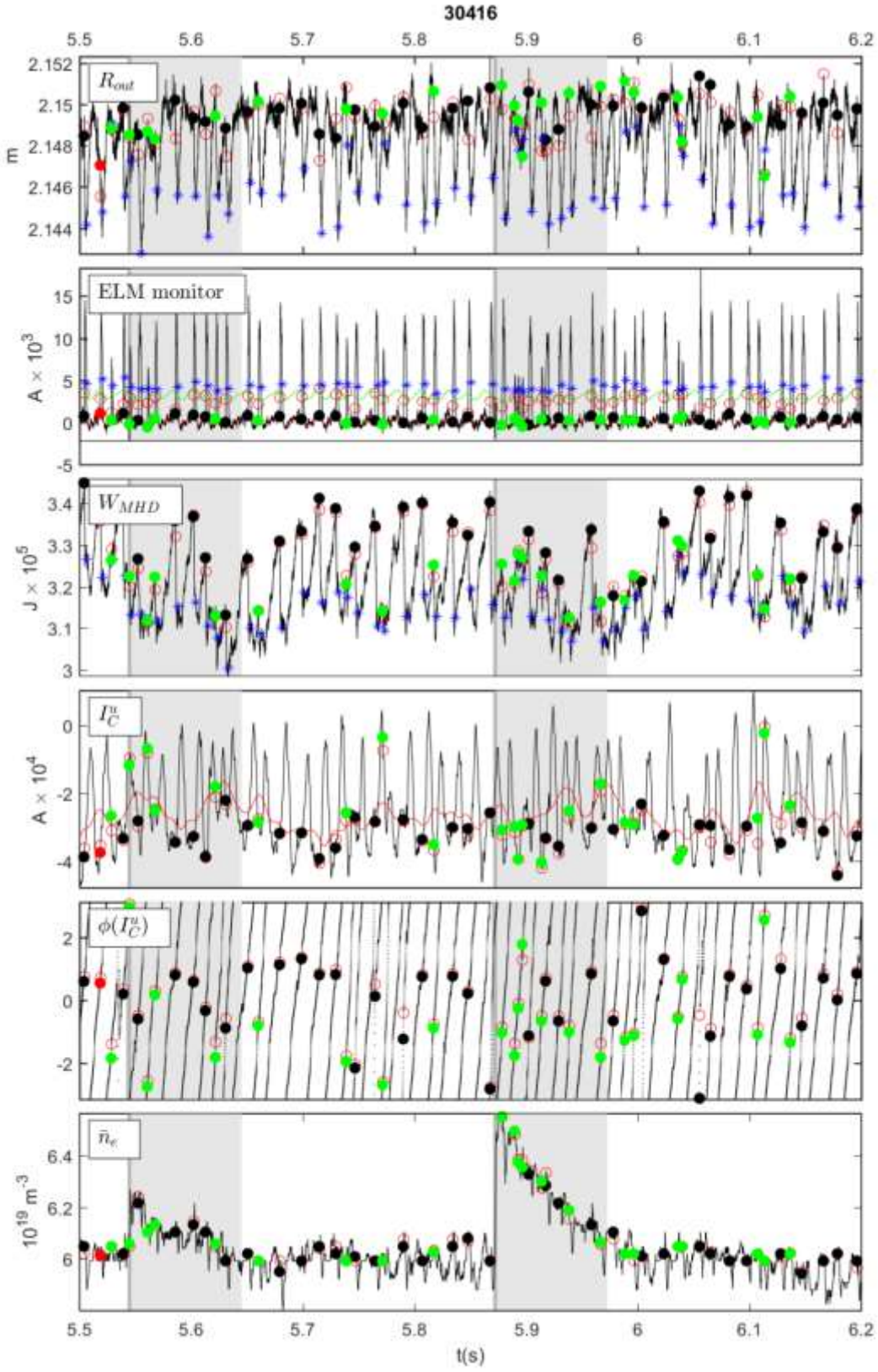

78

Overview of a time interval earlier in the same plasma for comparison. We plot in the same format as ED Figure 3 an interval of 0.7s duration from a time interval before the plasma transitions into synchronous dynamics. ELMs which generate an energy drop (in the WMHD signal) of $<10^4$ J are plotted with filled green circles, all other ELMs with black filled circles.

ED Figure 6

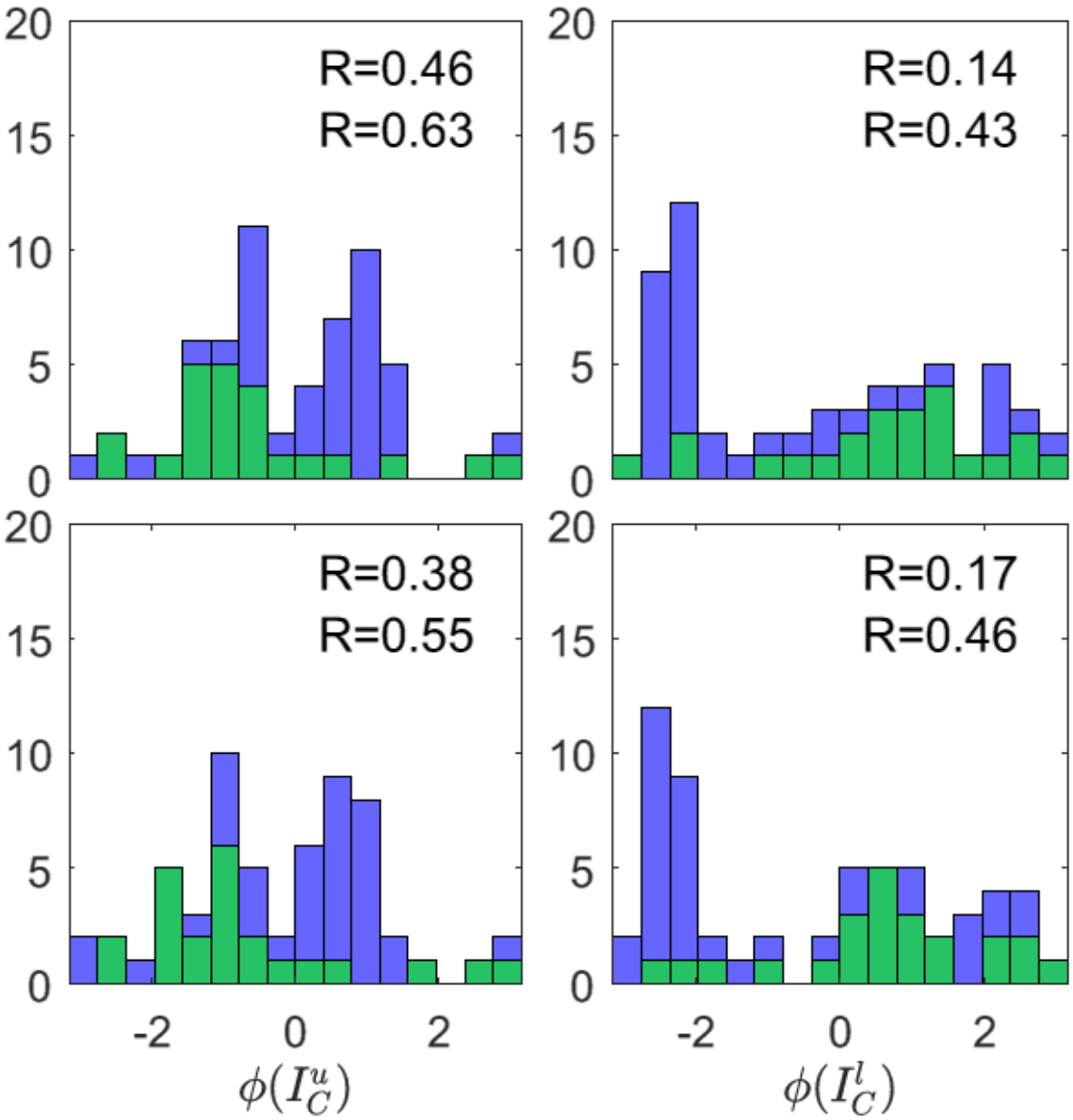

Histogram of the control system field coil phases at, and just before ELM onset for the interval plotted in ED Figure 5. The format is the same as in Figure 2 of the main paper except that ELMs which generate an energy drop (in the W_{MHD} signal) of $<10^4$ J are

89 overplotted with green bars. Rayleigh's R is calculated for all ELMs (upper R value) and only
90 large ELMs with energy drop $>10^4$ J (lower R value).

91 **ED Figure 7**

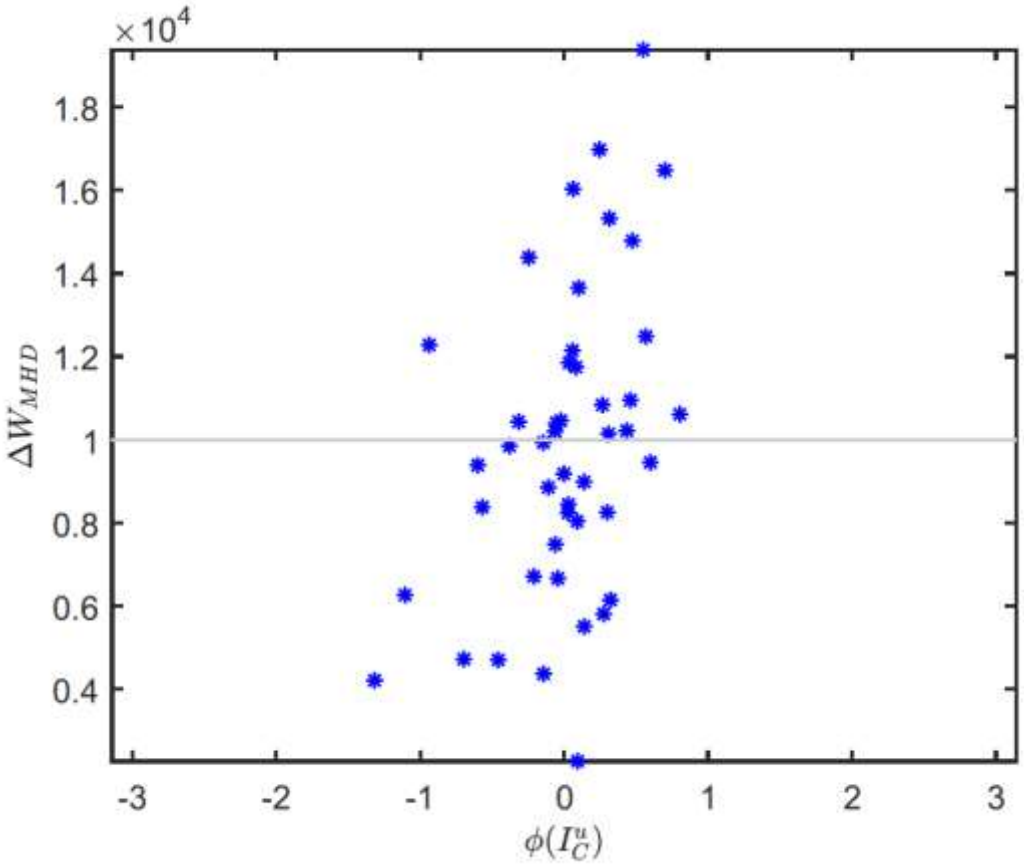

92

93 ELM energy release shows some dependence on I_C^u phase.